remote sensing

Article

A Decrease in the Daily Maximum Temperature during Global Warming Hiatus Causes a Delay in Spring Phenology in the China–DPRK–Russia Cross-Border Area

Minshu Su [1], Xiao Huang [2], Zhen Xu [2,*], Weihong Zhu [2] and Zhehao Lin [2]

[1] College of Intergration Science, Yanbian University, Yanji 133002, China; 2020010799@ybu.edu.cn
[2] College of Geography and Ocean Sciences, Yanbian University, Yanji 133002, China; 2019010414@ybu.edu.cn (X.H.); whzhu@ybu.edu.cn (W.Z.); zhlin@ybu.edu.cn (Z.L.)
* Correspondence: xuzhen@ybu.edu.cn; Tel.: +86-158-4433-2323

Abstract: Spring phenology is the most sensitive indicator of climate change and exploring its response to climate change has important implications for ecosystem processes in the study area. The temperature changes before and after the global warming hiatus may affect the spatiotemporal pattern of land surface phenology. In this paper, taking the China–DPRK (Democratic People's Republic of Korea)–Russia cross-border region as an example, based on GIMMS NDVI data, the Polyfit-Maximum method was used to extract the start date of the vegetation growing season (SOS). The variation trend of SOS and its response to climate change were analyzed in the early (1982–1998) and late (1998–2015) periods of the warming hiatus. At the regional scale, the spatial distribution of the SOS in the China–DPRK–Russia (CDR) cross-border area presents an elevation gradient, which is earlier in high-elevation areas and later in low-elevation areas. The temporal and spatial trend of SOS is mainly correlated by daytime maximum temperature (Tmax). The significant increase in Tmax in the early period promoted the advance of SOS (0.47 days/year), and the decrease in Tmax in the later period caused the delay of SOS (0.51 days/year). While the main influencing factor of the SOS changes in the region in the early and late periods was Tmax, the response of the SOS changes in China, DPRK and Russia to climate change also changed with the dramatic temperature changes during the warming hiatus. The Chinese side is increasingly responding to Tmax, while the North Korean side is becoming less responsive to climatic factors, and precipitation and radiation on the Russian side are driving the advance of the SOS.

Keywords: global warming hiatus; SOS; NDVI; climate change; China–DPRK–Russia border

check for updates

Citation: Su, M.; Huang, X.; Xu, Z.; Zhu, W.; Lin, Z. A Decrease in the Daily Maximum Temperature during Global Warming Hiatus Causes a Delay in Spring Phenology in the China–DPRK–Russia Cross-Border Area. *Remote Sens.* **2022**, *14*, 1462. https://doi.org/10.3390/rs14061462

Academic Editor: Cholho Song

Received: 15 January 2022
Accepted: 17 March 2022
Published: 19 March 2022

1. Introduction

Land surface phenology is a very useful approach; it uses time series of satellite sensor-derived vegetation indices to describe seasonal vegetation dynamics according to vegetation index time series [1,2]. It is also a phenomenon that recurs in a yearly cycle in the plant development stage [3]. It not only drives the key processes of vegetation growth (such as photosynthesis and transpiration), but also has important effects on the ecosystem carbon cycle, water cycle and nutrient cycle [4–9]. However, spring phenology is very sensitive to climate change [10]. Based on the phenology observation network [11–13], remote sensing monitoring [14,15] and phenology model simulation [16], it is agreed that global warming has caused the advance of SOS and the delay of the end date of the vegetation growing season (EOS). While the degree of advance of SOS varies in different regions [17–21], the advance of SOS is the main reason for the prolongation of the growing season of vegetation [22,23]. Spring phenology is influenced by a variety of climatic factors, which are often correlated [3]. As one of the important indicators to characterize the response of ecosystems to climate change, spring phenology is the most sensitive factor to climate change [3]. Therefore, accurate monitoring of temporal and spatial changes of

SOS and quantification of the response of SOS to various climatic factors are the basis for evaluating the response of nature to climate change and can also provide basic data for improving regional biological communities.

Temperature is one of the most important factors affecting SOS [24] because plants can only develop and grow under suitable temperatures, and a certain accumulated temperature can promote plants to complete their life cycle [25]. Therefore, accurate quantification of the effects of Tmax and Tmin on SOS is the basis for elucidating the sensitivity of SOS to temperature fluctuations. Previous studies have shown that SOS in the high latitudes of the Northern Hemisphere is mainly affected by Tmax due to the greater contribution of Tmax to the heat accumulation required for plant leaf emergence in spring [26]. At the regional scale, there are major differences. For example, the negative partial correlation between SOS and Tmin in the Qinghai-Tibet Plateau is stronger than the negative partial correlation between SOS and Tmax, which also indicates that the SOS in this region and other areas in the high latitudes of the Northern Hemisphere is less restricted by Tmax and radiation, which may be due to the low temperature reduction of constraints [27]. Besides temperature, precipitation also significantly alters the SOS [28,29]. It can be seen that the spatial heterogeneity of the limiting effect of climatic factors on SOS is large. While the world continues to warm, the global mean surface temperature (GMST) during 1998–2013 increased less than that of the second half of the 20th century. IPCC refers to 1997–1998 as the "global warming hiatus" [30,31]. Previous studies have shown that the phenological change rate slowed down from 1998 to 2012, and there was no significant change trend in SOS and EOS [30]. Most studies have briefly explained this trend as a result of weakened warming in spring or winter [32]. Hoonyoung also found the characteristics of the slowing down of the SOS promotion trend from 1982 to 2013 when studying the boreal forest. He finds that most of the reasons for the slowing down of this trend of the SOS are attributed to the slowing down of the warming trend, rather than the sensitivity changes of SOS to climate variables [33]. Wang et al. used five different methods to obtain the phenological data of the Northern Hemisphere around 1998 and found that the SOS was significantly advanced by 0.34 days/year before 1998, and the advance trend decreased to 0.02 days/year after 1998. The delay rate of the EOS was 0.26 days/year before 1998, but it showed an advanced trend after 1998 [34]. Therefore, it is particularly important to accurately quantify the influence effects of different climate factors on SOS before and after the warming hiatus.

Remote sensing technology provides new and effective means for phenological studies on landscape or larger scales. The phenological period extraction method based on remote sensing technology refers to constructing and reconstructing a time series through vegetation indices at multiple time points and extracting phenological information from the reconstructed time series [35]. Remote sensing monitoring is the most effective method to monitor the phenological in a long time series and a large area. Under the influence of climate change, it also realizes the analysis of dynamic temporal and spatial changes of phenology. The Normalized Differential Vegetation Index (NDVI) is the optimal indicator for vegetation growth status, vegetation coverage type and other information. It can accurately and sensitively reflect the vegetation growth season and photosynthesis intensity in a large coverage area, vegetation metabolic intensity and seasonal and interannual changes. It has good adaptability in time and space, so remote sensing methods based on NDVI time-series data occupy a very important position in the current common methods for monitoring vegetation phenological changes [36]. As a typical method for extracting SOS, the Polyfit-Maximum method has been widely used in different scale studies due to its good performance. Shen et al. used this method to extract the spring phenology of freshwater marshes in northeast China from 2001 to 2016 [37]. Piao also used this method to study the characteristics of spring phenology and autumn phenology in temperate grasslands in China from 1982 to 1999 [35]. Shen also used this method to calculate the spring phenology trend of temperate grassland vegetation in China from 1982 to 2015 [38].

While the research on the response between SOS and climate change is relatively mature, there are few studies on the regional scale in areas with obvious ecological and environmental differences across borders. Moreover, the understanding of the response relationship to climatic factors before and after the warming hiatus is still relatively fragmented. Therefore, this paper takes the CDR cross-border area as the research area, takes 1998 as the node of the warming hiatus to monitor the temporal and spatial trend of SOS in the border areas of the three countries and quantifies the climate factors (Tmax, Tmin, precipitation and radiation). This study provides the scientific basis and basic data for further exploration of ecological functions and measures to address climate change.

2. Materials and Methods

2.1. Study Area

The study area is located in the middle and high latitudes, 123° to 140°E and 37° to 49°N, covering a total area of 512,000 km^2, in three countries—China, DPRK, and Russia—including Jilin, Liaoning and the eastern Heilongjiang provinces of China, the whole of DPRK and Primorsky Krai in Russia (Figure 1). The Chinese area is in the mid-latitude region and has a temperate continental monsoon climate. Most of the vegetation types in the study area are forest, and the terrain is complex. DPRK is located on the north side of the Korean Peninsula, bordering China in the north and Russia in the northeast. There are more mountains and fewer plains. The main climate types are continental and maritime, belonging to the temperate continental monsoon climate. The Russian side is bordered on the west by China and a small part by DPRK. In winter, Binhai Krai is cold and dry under the influence of the cold air mass brought by the Mongolia–Siberia high from the Eurasian continent. Summer is influenced by the monsoon climate and the sea's moist airflow, which results in a mild and humid climate. As a whole, the terrain of the study area is mostly mountainous. It is warm and rainy in summer and cold and dry in winter. The average annual temperature is about 3.96 °C, and the annual precipitation is about 787.4 mm; the forest cover in the region is as high as 70 percent.

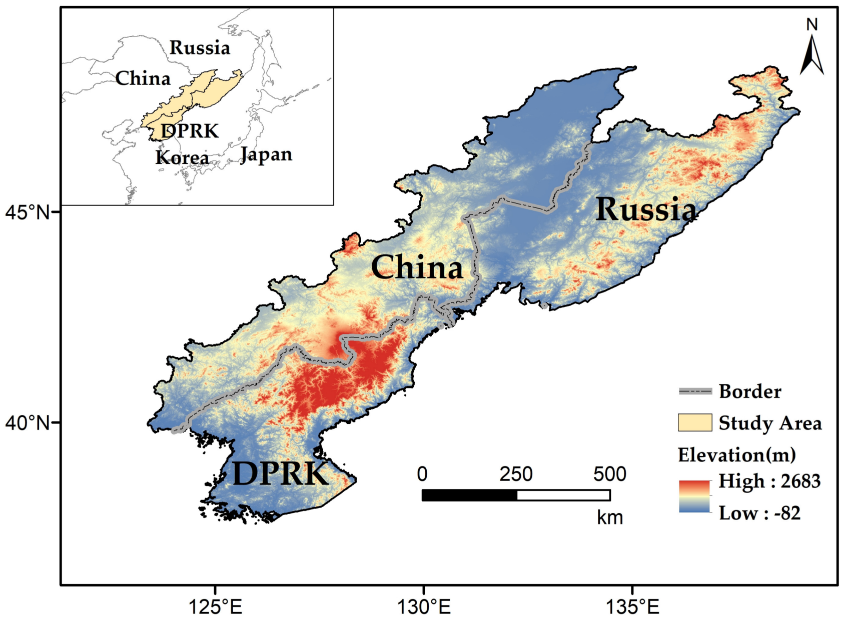

Figure 1. Geographical location and elevation of China–DPRK–Russia cross-border area.

2.2. Data

2.2.1. NDVI Data

The vegetation index data used in this study is the third-generation normalized vegetation index (GIMMS NDVI) published by NASA's Global Monitoring and Modeling Research Group (GIMMS) on the NOAA/AVHRR series of satellite sensors. The dataset has a spatial resolution of 1/12° × 1/12° (about 8 km), a temporal resolution of 15 days and a time range from January 1982 to December 2015 [14,39]. GIMMS NDVI data have been corrected to remove sensor degradation caused by volcanic eruptions, clouds and stratospheric aerosols for a range of off-stream effects [40]. The set is suitable for determining long-term trends in vegetation activity [41]. GIMMS NDVI3g V1 data acquisition website: https://ecocast.arc.nasa.gov/data/pub/gimms/3g.v1/ (accessed on 11 January 2022)

2.2.2. Climate Data

The climate data used in this study were obtained from TerraClimate, a high spatial resolution (1/24°, ~4 km) monthly climate and climatic water balance dataset of the global terrestrial surfaces from 1958 to 2015. It uses climatically aided interpolation to combine high-spatial-resolution climate normals from the WorldClim dataset with coarser-resolution time-varying (i.e., monthly) data from other sources to generate precipitation, Tmax, Tmin, wind speed, vapor pressure and solar radiation. Using this dataset, we calculated the average of the Tmax and Tmin for 12 months of each year. For precipitation and solar radiation, we calculated the sum of the 12 months of each year.

The elevation data used in this study is the SRTM DEM UTM 90M resolution digital elevation data product obtained from Geospatial Data Cloud.

2.3. Methods

2.3.1. Extraction of SOS

In this study, MATLAB software was used, and the Polyfit-Maximum method was used to determine the start date of the vegetation growing season (SOS) [35]; the principle of this method is to set the date of the maximum increase of NDVI as the start date of the growing season. Due to the accuracy of this method, a large number of studies have used this method to identify the SOS [38,39]. First, we calculated the multi-year mean of NDVI, obtained the NDVI time series with an interval of 15 days and then calculated the temporal change rate of NDVI according to Formula (1). The formula is as follows:

$$\mathrm{NDVIratio(t)} = \frac{\mathrm{NDVI(t+1)} - \mathrm{NDVI(t)}}{\mathrm{NDVI(t)}} \tag{1}$$

Here, t represents the interval of 15 days, and NDVI(t) represents the multi-year average NDVI value on the t day. When the NDVI ratio reaches the maximum value, the NDVI at this time is used as the NDVI threshold for evaluating the SOS to determine the average start date of vegetation greening.

As it is affected by some non-vegetation effects of cloud, atmosphere, solar radiation angle and other factors, the NDVI detected by remote sensing usually has some outliers. To reduce the impact of outliers on phenological assessment, we used the polynomial maximum method, where a sixth-degree polynomial was considered to better fit the NDVI time series. Its formula is as follows:

$$\mathrm{NDVI(t)} = \mathrm{a} + \mathrm{a_1 t^1} + \mathrm{a_2 t^2} + \mathrm{a_3 t^3} + \mathrm{a_4 t^4} + \mathrm{a_5 t^5} + \mathrm{a_6 t^6} \tag{2}$$

In the formula, NDVI(t) is the NDVI fitting value on the t day of the year, and a, a_1-a_6 are the fitting coefficients obtained by least square regression.

2.3.2. Trend Analysis

In addition, when analyzing the trends of SOS and climate variables at the regional scale and pixel scale, this paper adopts the univariate linear regression analysis method based on the least-squares method [37], and the calculation formula is:

$$\mathrm{SLOPE} = \frac{\mathrm{n} * \sum_{\mathrm{i}=1}^{\mathrm{n}} \mathrm{i} * \mathrm{P_i} - \left(\sum_{\mathrm{i}=1}^{\mathrm{n}} \mathrm{i}\right)\left(\sum_{\mathrm{i}=1}^{\mathrm{n}} \mathrm{P_i}\right)}{\mathrm{n} * \sum_{\mathrm{i}=1}^{\mathrm{n}} \mathrm{i}^2 - \left(\sum_{\mathrm{i}=1}^{\mathrm{n}} \mathrm{i}\right)^2} \tag{3}$$

In the formula, SLOPE represents the slope of the variable P regression equation, P_i is the variable value in the ith year, and n is the number of years in the study period. When SLOPE is positive, it means that the variable has an upward trend; when SLOPE is negative, it means that the variable shows a downward trend; the greater the absolute value of SLOPE, the greater the magnitude of the changing trend. When slope shows an upward trend, it means that the spring phenology is delayed. When slope shows a downward trend, it means that the spring phenology is advanced.

2.3.3. Correlation Analysis of SOS and Climate Factors

We used partial correlation analysis to analyze the correlation between Tmax, Tmin, precipitation and solar radiation and the SOS. When there is colinearity among multiple climate variables, partial correlation analysis can exclude the influence of other variables on SOS so as to explore the relationship between a single climate factor and SOS separately, which is an important reason for our choice of partial correlation analysis method. The calculation formula is:

$$r_{xy.z} = \frac{r_{xy} - r_{xz}r_{yz}}{\sqrt{\left(1 - r^2_{xy}\right)\left(1 - r^2_{yz}\right)}} \tag{4}$$

In the formula, $r_{xy.z}$ is the partial correlation coefficient between x and y after variable z is fixed; r_{xy} is the relationship between variable x and variable y; r_{yz} is the correlation coefficient between variable y and variable z; and r_{xz} is the difference between variable x and variable z.

For significance testing of the partial correlation coefficient, the *t*-test method is generally adopted, and the statistic calculation formula is as follows:

$$t = \frac{r_{xy.z}\sqrt{n - m - 1}}{\sqrt{1 - r^2_{xy.z}}} \tag{5}$$

In the formula, $r_{xy.z}$ is the partial correlation coefficient; m is the number of independent variables (m = 4). By comparing the critical values ta corresponding to different significance levels in the t-test distribution table, if t > ta, the partial correlation is significant; otherwise, if t < ta, the partial correlation is not significant. The critical value ta = 0.05 was selected; that is, $p < 0.05$ indicates a significant trend of change.

According to the results of partial correlation analysis, we take the climate factor with large absolute value of partial correlation coefficient with SOS as the main influence factor of the region; that is, it is considered that this climate factor has the greatest impact on the region.

3. Results and Discussion

3.1. The Spatiotemporal Pattern of Spring Phenology

As shown in Figure 2a, the spatial distribution map of the average start date of the vegetation growing season (SOS) from 1982 to 2015 was calculated based on pixels. The results showed that the SOS in this area was mainly concentrated between day 95 of the year (DOY) and 125 DOY (corresponding to 5 March to 5 April in leap years), and the average SOS occurred on 105 DOY. To compare the accuracy of the SOS extraction results, we compared with the results of Wang et al. Using the calculation results of Wang et al., the multi-year averages in the region from 1982 to 2014 were analyzed, and the calculation results were found to be similar [34]. The results of Wang et al. showed that the SOS in this region was mainly concentrated between 95 and 120 DOY, with an average of about 101.2 DOY. A comparison of the three regions (the Chinese side of the study area, the North Korean side and the Russian side) found that in the 34-year period from 1982 to 2015, the Russian side of the CDR cross-border area was the latest, about 111.4 DOY. The earliest SOS is on the North Korean side, about 100.1 DOY. China's SOS is close to that of North Korea, about 101.9 DOY. There is a relatively obvious distribution characteristic of elevation gradient, as shown in Figure 2b SOS is the earliest in the southwest region near the Northeast Plain, concentrated in 70 DOY to 90 DOY, while in the Changbai Mountain region and the northeast Sikhote Mountains with higher elevations, SOS is later, concentrated between 130 and 150 DOY. This is mainly because the vegetation needs a certain accumulated temperature before green-up [42], the temperature in low elevation areas is higher than that in high elevation areas, so the accumulated temperature in low elevation areas can be reached earlier to make the vegetation start greening. While the elevation in mountainous areas is high and the temperature is low, so it takes longer to reach the accumulated temperature [43].

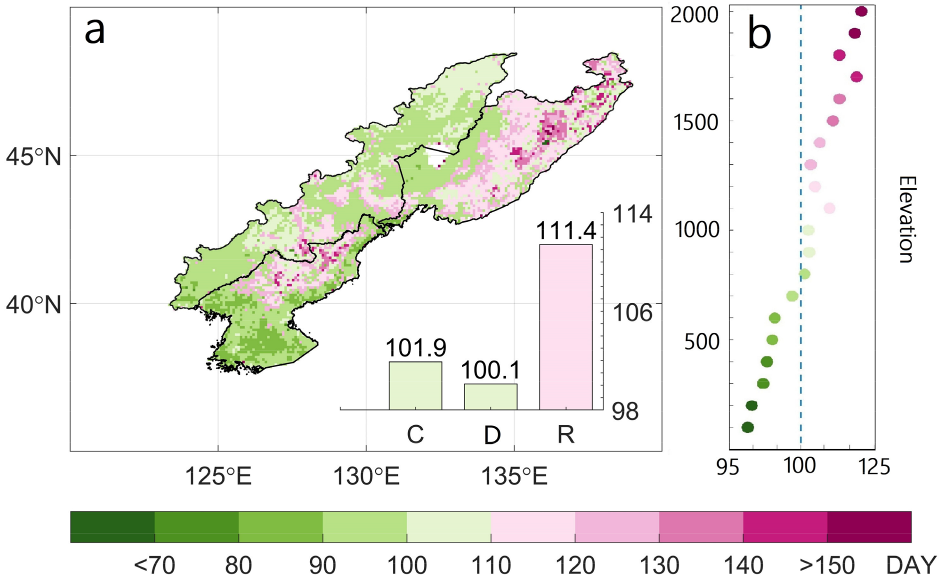

Figure 2. (**a**) Spatial distribution of multi-year mean value of SOS in the China (C), DPRK (D) and Russia (R) cross-border from 1982 to 2015; (**b**) Distribution of SOS along the elevation in the China–DPRK–Russia cross-border area.

To understand the variation of SOS at the regional scale, we analyzed the interannual fluctuation of SOS in the study area from 1982 to 2015. As shown in Figure 3a, the SOS showed a slight delay at the regional scale in the 34-year period from 1982 to 2015, and the inter-annual fluctuations were large, with a difference of nearly 33 days between the earliest and the latest (the earliest SOS occurred on 84 DOY in 1998, and the latest SOS occurred on 117 DOY in 2012). However, the interannual variation of SOS before and after the warming hiatus showed an opposite trend, with an advanced trend in the early stage (−0.47 days/year) and a delayed phenomenon in the later stage (0.51 days/year). For the three regions, the SOS changes before and after the warming hiatus all showed a trend of advancing first and then delaying. However, the rate of SOS delay in the later period was greater than that of the earlier period. Therefore, the SOS on the regional scale in the three regions showed a trend of delay in the 34-year period from 1982 to 2015. In the early period (1982–1998), the maximum SOS advance rate on the Russian side was about −0.7 days/year, and the Chinese and North Korea sides were about −0.39 days/year and −0.25 days/year, respectively. In the later period (1998–2015), the largest SOS delay rate was on the North Korean side, about 0.56 days/year, which was twice the SOS advance rate in the earlier period. The rate of SOS delay on the Russian side and the Chinese side is nearly the same, about 0.49 days/year and 0.48 days/year, respectively. Because we used linear regression, there is interference of outliers, although the linear trend is not very significant on the regional scale, but many pixels have a linear trend on the spatial scale.

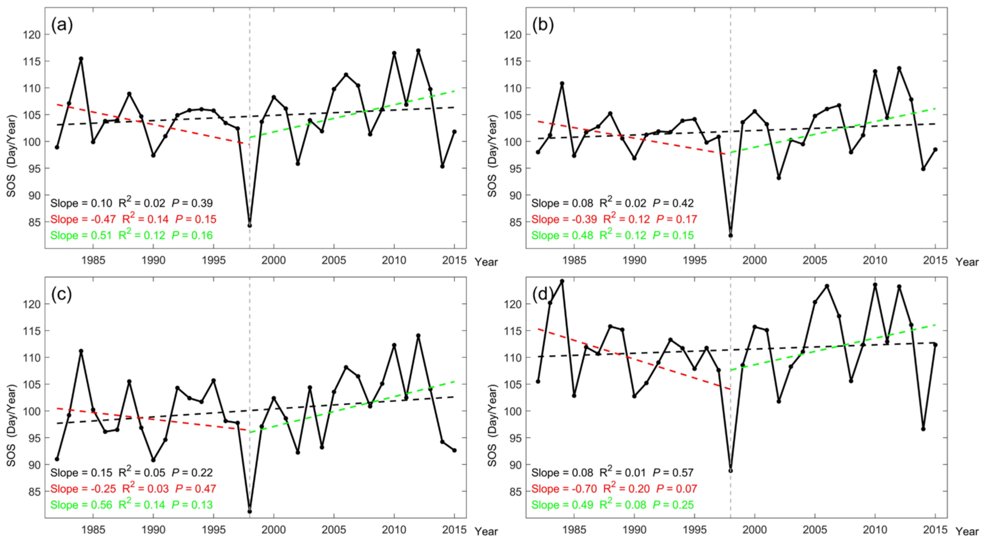

Figure 3. The inter-annual variation trend of SOS from 1982 to 2015. (**a**) China–DPRK–Russia cross-border area. (**b**) China side. (**c**) North Korean side. (**d**) Russian side. (The black solid black line represents the SOS annual series from 1982 to 2015, the red dashed line represents the interannual change trend from 1982 to 1998, and the green dashed line represents the inter-annual change trend from 1998 to 2015.).

In order to further analyze the temporal and spatial variation pattern of SOS, this paper adopts the temporal and spatial trend analysis of the interannual variation at the pixel scale. The results show that the SOS in the CDR cross-border area has not changed obviously on the spatial scale in the 34-year period from 1982 to 2015 (Figure 4c), and the spatial differences between the three regions are small.

However, the trend of SOS changes significantly before and after the warming hiatus. In the early stage, the vegetation SOS was advanced in a large area, the proportion of the advanced area was 88.8% (10.6%, $p < 0.05$) (Figure 4a) and the average advance rate was 0.56 days/year. The larger SOS advanced areas were mainly distributed in the northeast of the study area. The direction of the Sikhote Mountains (Russian side) and the central part of the study area are in the east of China's Heilongjiang Province. During this period, about 11.2% of the area showed a delayed greening period (0.5%, $p < 0.05$), which was mainly distributed in small areas on the South Korean side and the Changbai Mountains on the Chinese side. In the early stage, the SOS on the Russian side was significantly advanced, and about 96% of the regions showed an advance trend, with a rate of about −0.75 days/year. On the Chinese side, the SOS advance rate was about −0.45 days/year (92%), but the spatial difference is obvious. The central and southern regions had obvious advance trends, and the northern and central-south regions had no obvious changes. The southern region on the North Korean side experienced partial delays.

In the later stage, SOS showed a large area of delay; the proportion of delayed area was 60.2% (7.4%, $p < 0.05$), and the rate was about 0.49 days/year. The areas with more significant delays are the northernmost areas on the Chinese and Russian sides, namely Jiamusi City in Heilongjiang Province and the Primorsky Border Region. During this period, the SOS advance area was about 39.8% (3.1%, $p < 0.05$), and the rate was about −0.37 days/year. The most significant area of advance is the southern part of Liaoning Province, China, on the west side of the study area, with an advance rate of about −0.98 days/year. In the later period, the most significant area of SOS delay was the North Korean side, with about 68% of the area showing delay (0.52 days/year), followed by the Chinese side, except for the southern area (Dandong City, Liaoning Province) which continued to advance 0.37 days/year, the rest showed a delayed trend (63.2%, 0.44 days/year). On the Russian side, the significant delay area is the northern high-elevation area, and the delay rate was about 0.52 days/year. Before and after the warming hiatus, the area where the SOS changed from early to late accounted for 52.5% of the entire study area, mainly distributed on the North Korean side, the Chinese side (except the southwest), and the northern side of the Sikhote Mountains in Russia (Figure 4d).

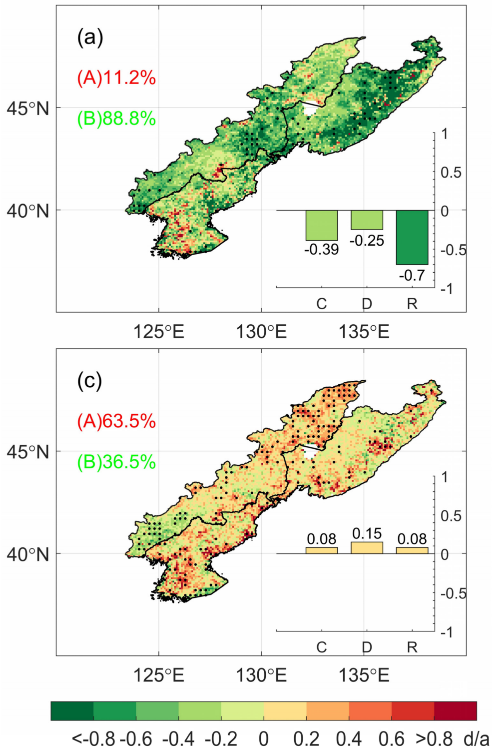

Figure 4. Spatial distribution of trend in SOS in the China–DPRK–Russia cross-border area. (**a**) Trend in SOS from 1982 to 1998. (**b**) Trend in SOS from 1998 to 2015. (**c**) Trend in SOS from 1982 to 2015. (**d**) Spatial distribution of SOS changed from advance trend to delay trend after 1998. The region with dots represents the sites with significant trend ($p < 0.05$).

The multi-year average value of vegetation rejuvenation period in the CDR cross-border generally shows the spatial distribution law of delaying from low-elevation areas to high-elevation areas, which is also basically consistent with the research results of the Qinghai Tibet Plateau [44,45], the United States [46,47] and Europe [48]. This is because the temperature gradually decreases with the increase in elevation, and the lower the temperature, the later the vegetation rejuvenation period, so the later the vegetation rejuvenation period in the highland [43]. It is observed that the amplitude of the advance trend from 1982 to 1998 increases with the increase in elevation. This upward trend in high-elevation areas shows that the difference of vegetation rejuvenation period between high-elevation areas and low-elevation areas has narrowed, which means that the contrast of spring phenology in the whole elevation gradient becomes weaker and weaker. From 1998 to 2015, the spring phenology in high-elevation areas was significantly delayed, which was contrary to the observation from 1982 to 1998. These two different trends offset each other before and after 1998, so the change trend of spring phenology from 1982 to 2015 is hardly affected by elevation.

In northern and alpine regions, temperature is considered to be the main factor affecting SOS [49]. From Figure 4, we can observe that due to the emergence of the global warming hiatus, there are two distinct trends of spring phenology in 1982–1998 and 1998–2015. From 1982 to 1998, Tmax and Tmin increased significantly at the rate of 0.056 °C/year and 0.055 °C/year, respectively, and then from 1998 to 2015, Tmax decreased at the rate of 0.013 °C/year, and the rising trend of Tmin also slowed down to 0.013 °C/year, making the spring phenology show the trend of advancing first and then delaying. Other scholars have also proved the impact of the global warming hiatus on phenology. A study by Jeong et al. (2011) shows that during the past decade, the promotion trend of spring vegetation restoration in some parts of Eurasia stagnated between the 1980s and 1990s [32].

3.2. Impact of Climate Change on SOS

Over a 34-year period from 1982 to 2015, the SOS in the CDR cross-border area was mainly correlated by temperature, and Tmax during the day had a greater impact on the SOS than Tmin at night (Figure 5o). This is because the SOS is more sensitive to the warming of Tmax than the warming of Tmin [38]. The partial correlation results showed that the SOS and Tmax in this area were negatively correlated in 97% of the pixels, of which 64% were significantly negatively correlated (Figure 5c). However, Tmin showed a significant positive correlation with SOS (Figure 5f), indicating that daytime warming and nighttime warming had asymmetric effects on SOS. That is, the rise of Tmax will lead to the advance of SOS, and the rise of Tmin will cause the delay of SOS. The effects of precipitation and radiation on the region were small; in particular, the partial correlation coefficient between precipitation and SOS was the smallest (Figure 5f). This is because the annual average precipitation in this area, which belongs to the humid area, is as high as 787.4 mm, and the SOS is more sensitive to temperature in the humid area, and the limiting effect of precipitation is not strong.

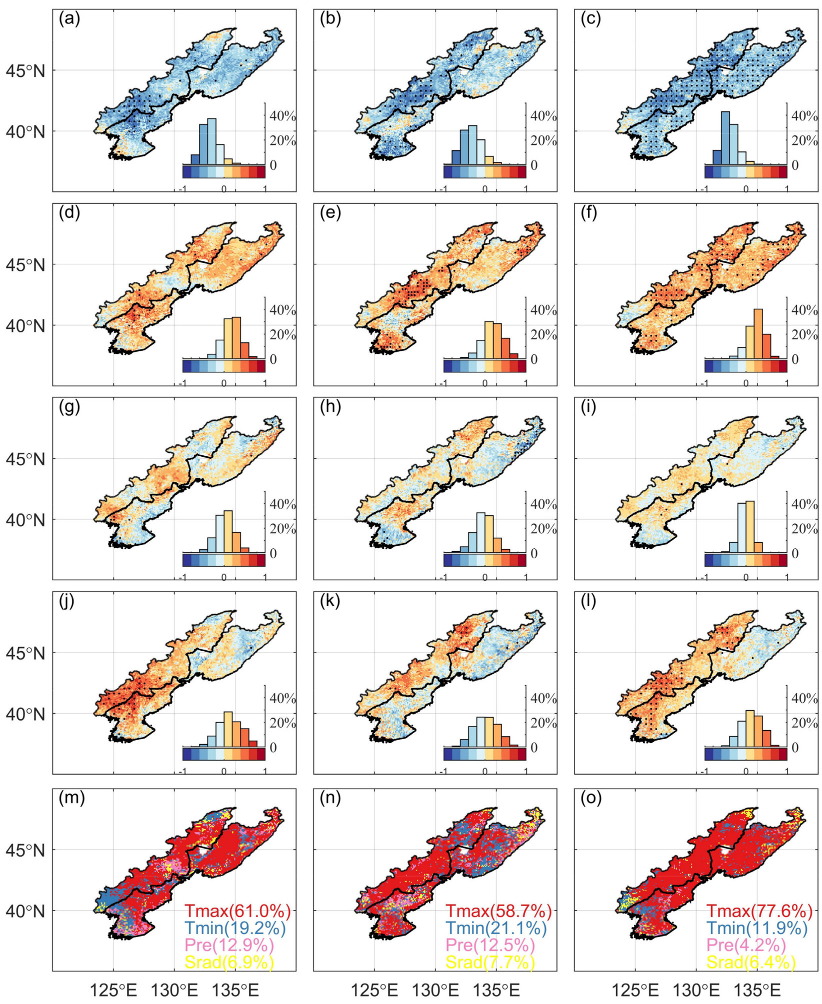

Figure 5. The response of SOS to changes in Tmax, Tmin, precipitation and solar radiation in the China–DPRK–Russia cross-border area. (**a**) Spatial distribution of the partial correlation coefficient between SOS and Tmax from 1982 to 1998. (**b**) Spatial distribution of the partial correlation coefficient between SOS and Tmax from 1998 to 2015. (**c**) Spatial distribution of the partial correlation coefficient between SOS and Tmax from 1982 to 2015. (**d**) Spatial distribution of the partial correlation coefficient

between SOS and Tmin from 1982 to 1998. (**e**) Spatial distribution of the partial correlation coefficient between SOS and Tmin from 1998 to 2015. (**f**) Spatial distribution of the partial correlation coefficient between SOS and Tmin from 1982 to 2015. (**g**) Spatial distribution of the partial correlation coefficient between SOS and precipitation from 1982 to 1998. (**h**) Spatial distribution of the partial correlation coefficient between SOS and precipitation from 1998 to 2015. (**i**) Spatial distribution of the partial correlation coefficient between SOS and precipitation from 1982 to 2015. (**j**) Spatial distribution of the partial correlation coefficient between SOS and solar radiation from 1982 to 1998. (**k**) Spatial distribution of the partial correlation coefficient between SOS and solar radiation from 1998 to 2015. (**l**) Spatial distribution of the partial correlation coefficient between SOS and solar radiation from 1982 to 2015. (**m**) Spatial distribution of the main climatic factors affecting SOS from 1982 to 1998. (**n**) Spatial distribution of the main climatic factors affecting SOS from 1998 to 2015. (**o**) Spatial distribution of the main climatic factors affecting SOS from 1982 to 2015. The region with dots represents the sites with significant trend ($p < 0.05$).

Before and after the warming hiatus, the main influence factors affecting the change of SOS changed slightly, the main influence climatic factor affecting the change of SOS in the study area was Tmax, and the proportion of Tmax playing a leading role in the early and late periods was still relatively high. In the early stage, the area with Tmax as the main influence factor accounted for 61%, while in the later period it dropped to 58.7%, but in the 34-year period from 1982 to 2015, the area with Tmax as the main influence factor accounted for as much as 77.6%. However, in the later period, Tmax in 88.2% of the regions showed a significant downward trend, which was the main reason for the significant delay of SOS in the later period. The increase in Tmax in the early stage caused a significant advance of SOS, while the decrease in the Tmax in the later stage caused a significant delay of SOS. Moreover, the rate of SOS delay is higher than the rate of SOS advance early in the warming hiatus, so Tmax in the 34-year period from 1982 to 2015 has caused the SOS to show a large-scale delay trend.

Tmin is also the main influence factor affecting SOS changes in local areas. For example, in the early stage, the main influence factor in the southwest direction of the study area was Tmin (Figure 5m), and the increase in Tmin in this area (Figure 6d) caused a significant advance of SOS (Figure 4a). Figure 4a–c show that the SOS shows a small area of persistent delay on the south side of the North Korean side, which is the result of the combined effect of Tmin and Tmax. The increase in Tmin in the early period caused the SOS delay in the region, while the decrease in Tmax in the later period caused the continuous delay of SOS in the region. In the northern part of the study area, the influence of Tmin became stronger and stronger, and the increase in Tmin in the region caused the delay of SOS in the region in the later period. All in all, before and after the warming hiatus, the main influence factor of SOS in this region was Tmax, while the influence of Tmin on SOS became stronger and stronger.

The SOS changes in the three regions before and after the warming hiatus were influenced by climatic factors, but the main influence factor was still Tmax. On the Chinese side, 80.5% of the area was influenced by temperature in the early stage, mainly in the central and northern regions. A total of 21.1% of the area was influenced by Tmin, mainly in the southern part (specific place name), which was influenced by Tmax in the later period. On the whole, the increase or decrease in Tmax during the day is the main factor affecting the change of SOS in this area.

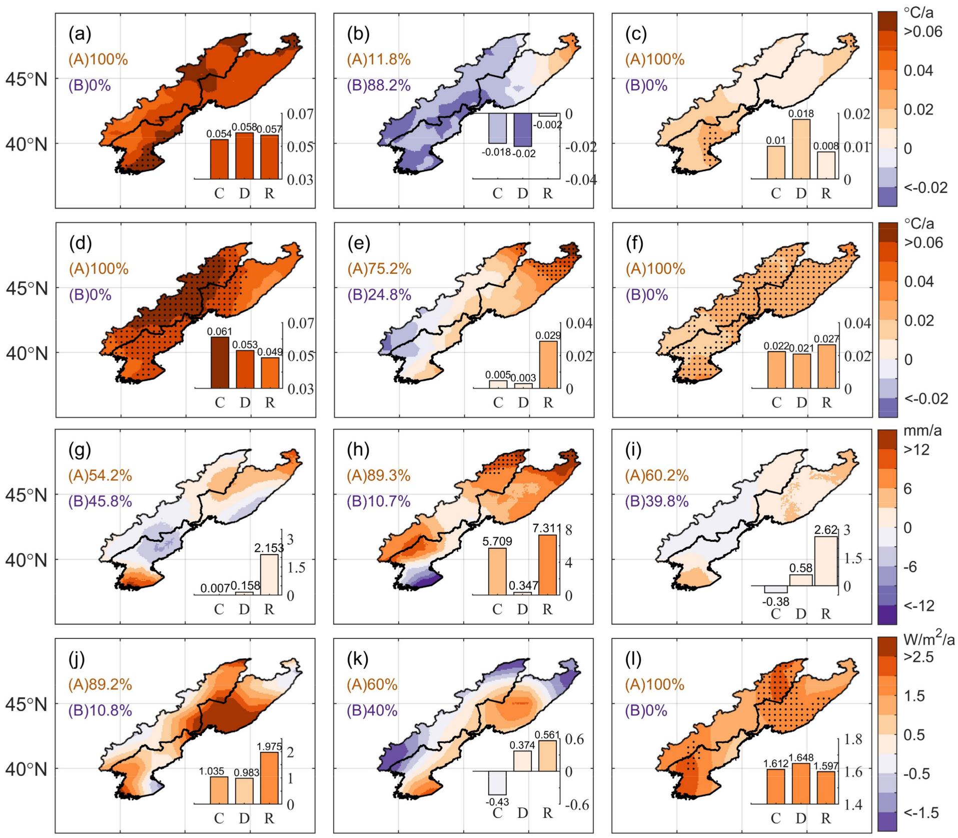

Figure 6. Spatial distribution of trend in Tmax, Tmin, precipitation and solar radiation in the China–DPRK–Russia cross-border area. (**a**) Trend in Tmax from 1982 to 1998. (**b**) Trend in Tmax from 1998 to 2015. (**c**) Trend in Tmax from 1982 to 2015. (**d**) Trend in Tmin from 1982 to 1998. (**e**) Trend in Tmin from 1998 to 2015. (**f**) Trend in Tmin from 1982 to 2015. (**g**) Trend in precipitation from 1982 to 1998. (**h**) Trend in precipitation from 1998 to 2015. (**i**) Trend in precipitation from 1982 to 2015. (**j**) Trend in solar radiation from 1982 to 1998. (**k**) Trend in solar radiation from 1998 to 2015. (**l**) Trend in solar radiation from 1982 to 2015. The region with dots represents the sites with significant trend ($p < 0.05$).

On the North Korean side, 48.9% of the area was affected by Tmax in the early stage, while 25.3% of the area was affected by Tmin. In the later period, nearly 53.8% of the area was affected by Tmax, the area with the Tmin affected factor decreased to 18.3%, and the trend of Tmin on the North Korean side was not obvious in the later period. On the whole, Tmax and Tmin jointly determine the SOS in this region. The increase in Tmax and Tmin causes the SOS to advance, and the decrease in Tmax causes the SOS to be delayed. However, it is worth noting that the partial correlation coefficients of SOS and climate factors on the North Korean side decreased in the later period, indicating that the degree of response of SOS to climate factors became smaller and smaller. This may be because, in the later period, due to the high influence of human factors, the large-scale development of land in North Korea led to the destruction of soil cover and vegetation. North Korea has the most degraded forests in the world, and extensive deforestation has caused natural disasters. The damage has increased significantly [50,51]. Natural vegetation is greatly affected by climate and environment. As a special type of land use, crops are greatly affected by human activities. Humans determine the sowing time of crops; at the beginning of the 21st century, the phenology of natural vegetation in China was about 20 days earlier than that of crops [52]. A large number of forests are converted to cultivated land in North Korea, which makes the SOS on the North Korean side fluctuate inconsistently with climate change, so the impact of climate change in the region is less than that of human activities [53].

On the Russian side, nearly 71.4% of the area was affected by Tmax in the early stage, and Tmax in most areas increased. In the later period, the area affected by Tmin increased from 12.8% to 30%, and the whole area on the Russian side showed an increasing trend. The increase rate was much higher than that on the North Korean and Chinese sides (Figure 6e). As shown in Table 1, Tmin has a greater impact on the SOS, so the continuous increase in Tmin is the main reason for the delay of the SOS in Russia in the later period. At the same time, the increase in precipitation and radiation promotes the delay of the SOS in this region.

Table 1. Partial correlation coefficient between SOS and different climatic factors and contribution of main influence climatic factors.

	Year	Tmax/Contribution	Tmin/Contribution	Pre/Contribution	Srad/Contribution
China	1982–1998	−0.36 (59.4%)	0.16 (21.1%)	0.08 (11.4%)	0.25 (8.1%)
	1998–2015	−0.40 (72.4%)	0.25 (15.5%)	0.03 (7.7%)	0.18 (4.5%)
	1982–2015	−0.45 (83.1%)	0.26 (9.2%)	0.05 (1.7%)	0.26 (6.0%)
DPRK	1982–1998	−0.32 (48.9%)	0.20 (25.3%)	−0.04 (19.9%)	0.22 (6.0%)
	1998–2015	−0.30 (53.8%)	0.13 (18.3%)	−0.02 (17.4%)	−0.06 (10.4%)
	1982–2015	−0.33 (65.7%)	0.19 (18.5%)	−0.02 (10.1%)	0.17 (5.7%)
Russia	1982–1998	−0.33 (71.4%)	0.19 (12.8%)	0.01 (9.6%)	−0.06 (6.2%)
	1998–2015	−0.25 (45.5%)	0.16 (30.0%)	−0.11 (14.7%)	−0.12 (9.9%)
	1982–2015	−0.39 (79.5%)	0.49 (10.2%)	−0.06 (2.9%)	−0.06 (7.3%)

The performances of Tmax and Tmin are also different in different seasons. Deng found, in his research on boreal forests, that Tmax has a greater impact on spring phenology in spring than Tmin, and there are seasonal differences; Tmax mainly affects SOS in spring, and Tmin has a greater impact in winter [54]. From Table 1, it can be seen that the effects of Tmax and Tmin on SOS are opposite, which is consistent with the results of Lin [55]; Tmax is negatively correlated with SOS in more than 80% of the places, while Tmin is positively correlated with SOS. By comparing the strength of the correlation between SOS and Tmax and Tmin, it is found that the spring phenology in the Northern Hemisphere is mainly triggered by daytime temperature rather than night-time temperature, whether from remote sensing observations or manipulative experiments [26,56]. This is consistent with the conclusion of this paper. Lin's study found that Tmin and Tmax play different roles in forcing and chilling. In cold regions, SOS is more closely related to Tmin, while in warm regions, SOS is more closely related to Tmax. Due to the relatively low temperature in Russia, the correlation between SOS and Tmin in this region was greater than that between SOS and Tmax from 1982 to 2015, and Tmin was the main reason for the delay of SOS on the Russian side (Table 1).

Most of the vegetation on the Chinese side belongs to temperate forests. Studies have found that, in the past 30 years, the temperature increase rate of the average Tmax in temperate forests is greater than that of the average Tmin, and the temperature difference between the Tmax and the Tmin is gradually increasing [57]. This is inconsistent with the IPCC report, which shows that Tmin is increasing faster than Tmax in most parts of the world and that the daily temperature difference is decreasing [29]. This may be due to the large-scale afforestation on the Chinese side during the 21st century [58], which has increased the forest density, thus making Tmax during the day higher than other regions, resulting in an increase in temperature difference, which makes the SOS tend to be delayed.

Vegetation and air temperature are interrelated. For example, studies have shown that the reduction of wetlands will affect temperature changes. The surface temperature increases during the day in most months, increases at night during the non-growing period and decreases during the day from July to September. During the growth period, the nighttime surface temperature decreased [54]. We found that the SOS in this area showed a delayed trend, which was not consistent with the global warming environment. This may be due to the fact that the increase in the Tmin in the study area was higher than that of the Tmax, which neutralized the effect of the highest temperature on SOS. As a result, there is a slight delay in SOS. Some studies have shown that pre-season temperature has a more significant impact on SOS [33,59]. In recent years, due to global warming, the fence effect of the westerly belt has weakened, and the Arctic cold air frequently moves southward in winter and spring, causing frequent cold waves in the middle and high latitudes of the Northern Hemisphere. It can be seen that global warming has a negative feedback on the temperature in winter and spring to a certain extent, so it is necessary to conduct further seasonal studies on the surface temperature, but this cannot be realized due to limited data.

It should be noted that the current research may have some limitations. We did not distinguish land surface phenology according to different vegetation types. While most of the area is forest, it also includes grassland, cultivated land, wetland and construction land. In different vegetation types, vegetation phenology has its own characteristics and there are some differences in response to climate. Because we mainly studied land surface phenology, it fails to specifically analyze the differences between different vegetation types. In addition to SOS, EOS and growing season length should also be investigated in order to comprehensively use data to investigate phenological changes in the region under future climate change. In addition, the change trend of phenology calculated only by linear regression may be too single; some interannual variations may not be linear; we need to test it with a more robust non-parametric approach to trend analysis. Some studies have found that pre-season climate may have a greater impact on phenology [32,33], and there may be some limitations in only studying the average annual value of climate factors. Finally, considering the inaccuracy of satellite data and remote sensing estimation of vegetation phenology, we still need to verify the phenological results of the current study area by using the situ data.

4. Conclusions

The results of this paper show that the variation of SOS is affected by Tmax. The CDR cross-border area has experienced drastic climate change in the 34-year period from 1982 to 2015, with Tmax and Tmin dropping significantly in the later period of the warming hiatus. This led to a significant advance of SOS in the early vegetation in the area, but a large area of SOS was delayed in the later years. This reversal was mainly caused by a decrease in Tmax. While the spatial distribution of SOS shows the law of elevation gradient distribution, the influence of elevation is not very obvious on the change trend of SOS. This conclusion also emphasizes the value of accurately describing the relationship of temperature changes in vegetation growth under the influence of future climate change. In addition, the results of this study also show that there are obvious differences in the three regions of China, North Korea and Russia. In the early stage, the SOS in the three regions is affected by temperature (Tmax on the Chinese side, Tmax and Tmin on the North Korean side and the Tmin in Russia). In the later period, the responses of the three regions to climate change were quite different. The SOS on the Chinese side has an increasingly strong response to Tmax, and the Russian side has an increasingly complex response to climate change, with increased effects of precipitation and radiation. North Korea, on the other hand, showed an increasingly weakened relationship to climate change, and the impact of climate change on vegetation SOS on the North Korean side became less and less important, indicating that the change in SOS in the region may be affected by other factors, such as human activities, etc. In regional or global vegetation dynamic models, the impact of climate change and human activities on vegetation growth should be explicitly considered.

While, during the study period, the Terra Climate dataset showed that there were dramatic changes in temperature before and after the warming hiatus in the region, and the resulting SOS trend reversed, there are, however, still uncertainties in the study of the intermittent period of warming. In future studies, comparisons between various climate data and verification based on observational data should be carried out to evaluate the climate change in this region more accurately. In addition, this study only considered the changes of SOS, but vegetation growth is very complex. Therefore, it is necessary to comprehensively consider multiple factors in vegetation growth in future research, such as SOS, the end date of vegetation growing season (EOS), vegetation coverage, vegetation productivity and respiration. Overall, this study clarifies the temporal and spatial variation of SOS at the regional scale and elucidates the response to climate change. Therefore, this study has a high theoretical significance for the protection and sustainable development of the ecosystem in this region in the future.

Author Contributions: Conceptualization, Z.X. and M.S.; methodology, M.S. and X.H.; software, X.H.; validation, Z.X., Z.L. and W.Z.; formal analysis, M.S.; investigation, M.S.; resources, Z.X.; data curation, M.S. and X.H.; writing—original draft preparation, M.S.; writing—review and editing, Z.X., X.H., W.Z. and Z.L.; visualization, M.S.; supervision, Z.X.; project administration, Z.X.; funding acquisition, Z.X. All authors have read and agreed to the published version of the manuscript.

Funding: This research was funded by National Natural Science Foundation of China (grant number 41806227, 4197071437). The APC was funded by National Space Science Center (YS-2021-07-01-06).

Data Availability Statement: Not applicable.

Acknowledgments: This study was supported by National Natural Science Foundation of China (grant number 41806227, 4197071437) and National Space Science Center (YS-2021-07-01-06).

Conflicts of Interest: The authors declare no conflict of interest.

References

1. Henebry, G.M.; Beurs, K.M.D. *Remote Sensing of Land Surface Phenology: A Prospectus*; Springer: Dordrecht, The Netherlands, 2013; pp. 385–411.
2. Rodriguez-Galiano, V.F.; Dash, J.; Atkinson, P.M. Characterising the Land Surface Phenology of Europe Using Decadal MERIS Data. *Remote Sens.* **2015**, *7*, 9390–9409. [CrossRef]
3. Piao, S.; Liu, Q.; Chen, A.; Janssens, I.; Fu, Y.; Dai, J.; Liu, L.; Lian, X.; Shen, M.; Zhu, X. Plant phenology and global climate change: Current progresses and challenges. *Glob. Chang. Biol.* **2019**, *25*, 1922–1940. [CrossRef] [PubMed]
4. Myneni, R.; Keeling, C.D.; Tucker, C.J.; Asrar, G.; Nemani, R. Increased plant growth in the northern high latitudes from 1981 to 1991. *Nature* **1997**, *386*, 698–702. [CrossRef]
5. Jochner, S.; Menzel, A. Does flower phenology mirror the slowdown of global warming? *Ecol. Evol.* **2015**, *5*, 2284–2295. [CrossRef]
6. Pearson, R.G.; Phillips, S.J.; Loranty, M.M.; Beck, P.S.A.; Damoulas, T.; Knight, S.J.; Goetz, S.J. Shifts in Arctic vegetation and associated feedbacks under climate change. *Nat. Clim. Chang.* **2013**, *3*, 673–677. [CrossRef]
7. Thackeray, S.J.; Henrys, P.A.; Hemming, D.; Bell, J.R.; Botham, M.S.; Burthe, S.; Helaouët, P.; Johns, D.G.; Jones, I.D.; Leech, D.I.; et al. Phenological sensitivity to climate across taxa and trophic levels. *Nature* **2016**, *535*, 241–245. [CrossRef]
8. Zeng, Z.; Piao, S.; Li, L.Z.X.; Zhou, L.; Ciais, P.; Wang, T.; Li, Y.; Lian, X.; Wood, E.F.; Friedlingstein, P.; et al. Climate mitigation from vegetation biophysical feedbacks during the past three decades. *Nat. Clim. Chang.* **2017**, *7*, 432–436. [CrossRef]
9. Lang, W.; Chen, X.; Qian, S.; Liu, G.; Piao, S. A new process-based model for predicting autumn phenology: How is leaf senescence controlled by photoperiod and temperature coupling? *Agric. For. Meteorol.* **2019**, *268*, 124–135. [CrossRef]
10. Schwartz, M.D. Green-wave phenology. *Nature* **1998**, *394*, 839–840. [CrossRef]
11. Ahas, R.; Jaagus, J.; Aasa, A. The phenological calendar of Estonia and its correlation with mean air temperature. *Int. J. Biometeorol.* **2000**, *44*, 159–166. [CrossRef]
12. Menzel, A.; Fabian, P. Growing season extended in Europe. *Nature* **1999**, *397*, 659. [CrossRef]
13. Peñuelas, J.; Filella, I. Responses to a Warming World. *Science* **2001**, *294*, 793–795. [CrossRef]
14. Tucker, C.J.; Slayback, D.; Pinzon, J.E.; Los, S.; Myneni, R.; Taylor, M.G. Higher northern latitude normalized difference vegetation index and growing season trends from 1982 to 1999. *Int. J. Biometeorol.* **2001**, *45*, 184–190. [CrossRef]
15. Zhou, L.; Tucker, C.J.; Kaufmann, R.K.; Slayback, D.; Shabanov, N.V.; Myneni, R.B. Variations in northern vegetation activity inferred from satellite data of vegetation index during 1981 to 1999. *J. Geophys. Res. Atmos.* **2001**, *106*, 20069–20083. [CrossRef]
16. Lucht, W.; Prentice, I.C.; Myneni, R.B.; Sitch, S.; Friedlingstein, P.; Cramer, W.; Bousquet, P.; Buermann, W.; Smith, B. Climatic Control of the High-Latitude Vegetation Greening Trend and Pinatubo Effect. *Science* **2002**, *296*, 1687–1689. [CrossRef]
17. Kimball, J.S.; McDonald, K.C.; Running, S.W.; Frolking, S.E. Satellite radar remote sensing of seasonal growing seasons for boreal and subalpine evergreen forests. *Remote Sens. Environ.* **2004**, *90*, 243–258. [CrossRef]
18. Keeling, C.D.; Chin, J.F.S.; Whorf, T.P. Increased activity of northern vegetation inferred from atmospheric CO_2 measurements. *Nature* **1996**, *382*, 146–149. [CrossRef]
19. Fitter, A.H.; Fitter, R.S.R. Rapid Changes in Flowering Time in British Plants. *Science* **2002**, *296*, 1689–1691. [CrossRef]
20. Roetzer, T.; Wittenzeller, M.; Haeckel, H.; Nekovar, J. Phenology in central Europe-differences and trends of spring phenophases in urban and rural areas. *Int. J. Biometeorol.* **2000**, *44*, 60–66. [CrossRef]

21. Menzel, A.; Estrella, N.; Fabian, P. Spatial and temporal variability of the phenological seasons in Germany from 1951 to 1996. *Glob. Change Biol.* **2001**, *7*, 657–666.
22. Sparks, T.H.; Roy, D.B.; Dennis, R.L.H. The influence of temperature on migration of Lepidoptera into Britain. *Glob. Chang. Biol.* **2005**, *11*, 507–514. [CrossRef]
23. Chmielewski, F.-M.; Müller, A.; Bruns, E. Climate changes and trends in phenology of fruit trees and field crops in Germany, 1961–2000. *Agric. For. Meteorol.* **2004**, *121*, 69–78. [CrossRef]
24. Richardson, A.D.; Bailey, A.S.; Denny, E.G.; Martin, C.W.; O'Keefe, J. Phenology of a northern hardwood forest canopy. *Glob. Chang. Biol.* **2006**, *12*, 1174–1188. [CrossRef]
25. Xin-Bo, Z.; Jian-Ru, R.; Dan-Er, Z. Phenological observations onLarix principis-rupprechtii Mayr. in primary seed orchard. *J. For. Res.* **2001**, *12*, 201–204. [CrossRef]
26. Piao, S.; Tan, J.; Chen, A.; Fu, Y.; Ciais, P.; Liu, Q.; Janssens, I.; Vicca, S.; Zeng, Z.; Jeong, S.-J.; et al. Leaf onset in the northern hemisphere triggered by daytime temperature. *Nat. Commun.* **2015**, *6*, 6911. [CrossRef]
27. Shen, M.; Piao, S.; Chen, X.; An, S.; Fu, Y.H.; Wang, S.; Cong, N.; Janssens, I.A. Strong impacts of daily minimum temperature on the green-up date and summer greenness of the Tibetan Plateau. *Glob. Chang. Biol.* **2016**, *22*, 3057–3066. [CrossRef]
28. Li, R.; Luo, T.; Mölg, T.; Zhao, J.; Li, X.; Cui, X.; Du, M.; Tang, Y. Leaf unfolding of Tibetan alpine meadows captures the arrival of monsoon rainfall. *Sci. Rep.* **2016**, *6*, 20985. [CrossRef]
29. Shen, M.; Zhang, G.; Cong, N.; Wang, S.; Kong, W.; Piao, S. Increasing altitudinal gradient of spring vegetation phenology during the last decade on the Qinghai-Tibetan Plateau. *Agric. For. Meteorol.* **2014**, *189*, 71–80. [CrossRef]
30. Yan, X.; Boyer, T.; Trenberth, K.; Karl, T.R.; Xie, S.; Nieves, V.; Tung, K.; Roemmich, D. The global warming hiatus: Slowdown or redistribution? *Earth's Future* **2016**, *4*, 472–482. [CrossRef]
31. IPCC. *Climate Change 2013: The Physical Science Basis. Contribution of Working Group I to the Fifth Assessment Report of the Intergovernmental Panel on Climate Change*; Cambridge Univ. Press: Cambridge, UK, 2013; 1535p.
32. Jeong, S.J.; Chang-Hoi, H.O.; Gim, H.J.; Brown, M.E. Phenology shifts at start vs. end of growing season in temperate vegetation over the northern hemisphere for the period 1982–2008. *Glob. Change Biol.* **2011**, *17*, 2385–2399. [CrossRef]
33. Park, H.; Jeong, S.-J.; Ho, C.-H.; Park, C.-E.; Kim, J. Slowdown of spring green-up advancements in boreal forests. *Remote Sens. Environ.* **2018**, *217*, 191–202. [CrossRef]
34. Wang, X.; Xiao, J.; Li, X.; Cheng, G.; Ma, M.; Zhu, G.; Arain, M.A.; Black, T.A.; Jassal, R.S. No trends in spring and autumn phenology during the global warming hiatus. *Nat. Commun.* **2019**, *10*, 1–10. [CrossRef]
35. Piao, S.; Fang, J.; Zhou, L.; Ciais, P.; Zhu, B. Variations in satellite-derived phenology in China's temperate vegetation. *Glob. Change Biol.* **2006**, *12*, 672–685. [CrossRef]
36. Shen, X.; Liu, B.; Jiang, M.; Wang, Y.; Wang, L.; Zhang, J.; Lu, X. Spatiotemporal Change of Marsh Vegetation and Its Response to Climate Change in China From 2000 to 2019. *J. Geophys. Res. Biogeosci.* **2021**, *126*, e2020JG006154. [CrossRef]
37. Shen, X.; Liu, B.; Xue, Z.; Jiang, M.; Lu, X.; Zhang, Q. Spatiotemporal variation in vegetation spring phenology and its response to climate change in freshwater marshes of Northeast China. *Sci. Total Environ.* **2019**, *666*, 1169–1177. [CrossRef]
38. Shen, X.; Liu, B.; Henderson, M.; Wang, L.; Wu, Z.; Wu, H.; Jiang, M.; Lu, X. Asymmetric effects of daytime and nighttime warming on spring phenology in the temperate grasslands of China. *Agric. For. Meteorol.* **2018**, *259*, 240–249. [CrossRef]
39. Zhou, L.; Kaufmann, R.K.; Tian, Y.; Myneni, R.B.; Tucker, C.J. Relation between interannual variations in satellite measures of northern forest greenness and climate between 1982 and 1999. *J. Geophys. Res. Atmos.* **2003**, *108*, ACL-3. [CrossRef]
40. Myneni, R.B.; Dong, J.; Tucker, C.J.; Kaufmann, R.K.; Kauppi, P.E.; Liski, J.; Zhou, L.; Alexeyev, V.; Hughes, M.K. A large carbon sink in the woody biomass of Northern forests. *Proc. Natl. Acad. Sci. USA* **2001**, *98*, 14784–14789. [CrossRef]
41. Slayback, D.A.; Pinzon, J.E.; Los, S.O.; Tucker, C.J. Northern hemisphere photosynthetic trends 1982–99. *Glob. Chang. Biol.* **2003**, *9*, 1–15. [CrossRef]
42. Shen, M.; Tang, Y.; Chen, J.; Zhu, X.; Zheng, Y. Influences of temperature and precipitation before the growing season on spring phenology in grasslands of the central and eastern Qinghai-Tibetan Plateau. *Agric. For. Meteorol.* **2011**, *151*, 1711–1722. [CrossRef]
43. Piao, S.; Cui, M.; Chen, A.; Wang, X.; Ciais, P.; Liu, J.; Tang, Y. elevation and temperature dependence of change in the spring vegetation green-up date from 1982 to 2006 in the Qinghai-Xizang Plateau. *Agric. For. Meteorol.* **2011**, *151*, 1599–1608. [CrossRef]
44. Ma, X.; Zhen, S.; Deng, J.; Feng, Q.; Huang, X. Vegetationphenology dynamics and its response to climate changeon the Tibetan Plateau. *Acta Prataculturae Sin.* **2016**, *25*, 13–21.
45. Li Liu, L.; Zhang, Y.; Ding, M.; Li, S.; Chen, Q. Elevation-dependent alpine grassland phenology on the Tibetan Plateau. *Geogr. Res.* **2017**, *36*, 26–36.
46. Wang, H.; Ge, Q.; Dai, J.; Tao, Z. Geographical pattern in first bloom variability and its relation to temperature sensitivity in the USA and China. *Int. J. Biometeorol.* **2014**, *59*, 961–969. [CrossRef]
47. Cayan, D.R.; Dettinger, M.D.; Kammerdiener, S.A.; Caprio, J.M.; Peterson, D.H. Changes in the Onset of Spring in the Western United States. *Bull. Am. Meteorol. Soc.* **2001**, *82*, 399–415. [CrossRef]
48. Lin, S.; Ge, Q.; Wang, H. Spatiotemporal change in leaf-out phenology of typicalEuropean tree species and its response to climate change. *Chin. J. Appl. Ecol.* **2021**, *32*, 788–798.
49. Picard, G.; Quegan, S.; Delbart, N.; Lomas, M.R.; Toan, T.; Woodward, F.I. Bud-burst modelling in Siberia and its impact on quantifying the carbon budget. *Glob. Chang. Biol.* **2005**, *11*, 2164–2176. [CrossRef]

50. Zheng, D.; Wallin, D.O.; Hao, Z. Rates and patterns of landscape change between 1972 and 1988 in the Changbai Mountain area of China and North Korea. *Landsc. Ecol.* **1997**, *12*, 241–254. [CrossRef]
51. Tang, L.; Shao, G.; Piao, Z.; Dai, L.; Jenkins, M.A.; Wang, S.; Wu, G.; Wu, J.; Zhao, J. Forest degradation deepens around and within protected areas in East Asia. *Biol. Conserv.* **2010**, *143*, 1295–1298. [CrossRef]
52. Lu, P.; Yu, Q.; He, Q. Plant Phenology Response to Climate Change. *Acta Ecol. Sin.* **2006**, *26*, 923–929.
53. Zhang, H.; Li, Q.; Liu, J.; Shang, J.; Du, X.; Zhao, L.; Wang, N.; Dong, T. Crop classification and acreage estimation in North Korea using phenology features. *GIScience Remote Sens.* **2017**, *54*, 1–26. [CrossRef]
54. Deng, G.; Zhang, H.; Guo, X.; Shan, Y.; Ying, H.; Rihan, W.; Li, H.; Han, Y. Asymmetric Effects of Daytime and Nighttime Warming on Boreal Forest Spring Phenology. *Remote Sens.* **2019**, *11*, 1651. [CrossRef]
55. Meng, L.; Zhou, Y.; Li, X.; Asrar, G.R.; Mao, J.; Wanamaker, A.D.; Wang, Y. Divergent responses of spring phenology to daytime and nighttime warming. *Agric. For. Meteorol.* **2019**, *281*, 107832. [CrossRef]
56. Fu, Y.H.; Liu, Y.; De Boeck, H.J.; Menzel, A.; Nijs, I.; Peaucelle, M.; Peñuelas, J.; Piao, S.; Janssens, I. Three times greater weight of daytime than of night-time temperature on leaf unfolding phenology in temperate trees. *New Phytol.* **2016**, *212*, 590–597. [CrossRef]
57. Zhang, H.; Jin, Y.; Shen, X.; Li, G.; Zhou, D. Rising Air Temperature and Its Asymmetry under Different Vegetation Regions in China. *Sci. Geogr. Sin.* **2018**, *38*, 272–283.
58. Zhang, P.; Shao, G.; Zhao, G.; Le Master, D.C.; Parker, G.R.; Dunning, J.B., Jr.; Li, Q. China's forest policy for the 21st century. *Science* **2000**, *288*, 2135–2136. [CrossRef]
59. Wang, X.; Piao, S.; Xu, X.; Ciais, P.; MacBean, N.; Myneni, R.B.; Li, L. Has the advancing onset of spring vegetation green-up slowed down or changed abruptly over the last three decades? *Glob. Ecol. Biogeogr.* **2015**, *24*, 621–631. [CrossRef]